Journal Pre-proof

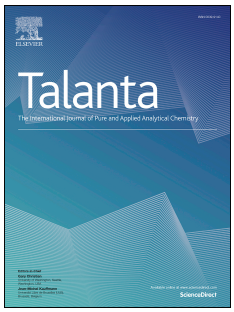

Microfluidic fluorescence biosensor for quantitative detection of HER2 in serum using an antibody–aptamer sandwich assay

J.P. Conde, M.R.V.C. Pinho, M.S.M. Mendes, I. Agostinho, R.G. Rodrigues, F.A. e Silva, M.G. Freire, V. Chu

PII: S0039-9140(26)00732-0

DOI: https://doi.org/10.1016/j.talanta.2026.130076

Reference: TAL 130076

To appear in: *Talanta*

Received Date: 20 March 2026

Revised Date: 12 May 2026

Accepted Date: 1 June 2026

Please cite this article as: J.P. Conde, M.R.V.C. Pinho, M.S.M. Mendes, I. Agostinho, R.G. Rodrigues, F.A. e Silva, M.G. Freire, V. Chu, Microfluidic fluorescence biosensor for quantitative detection of HER2 in serum using an antibody–aptamer sandwich assay, *Talanta*, https://doi.org/10.1016/j.talanta.2026.130076.

Microfluidic fluorescence biosensor for quantitative detection of HER2 in serum using an antibody–aptamer sandwich assay

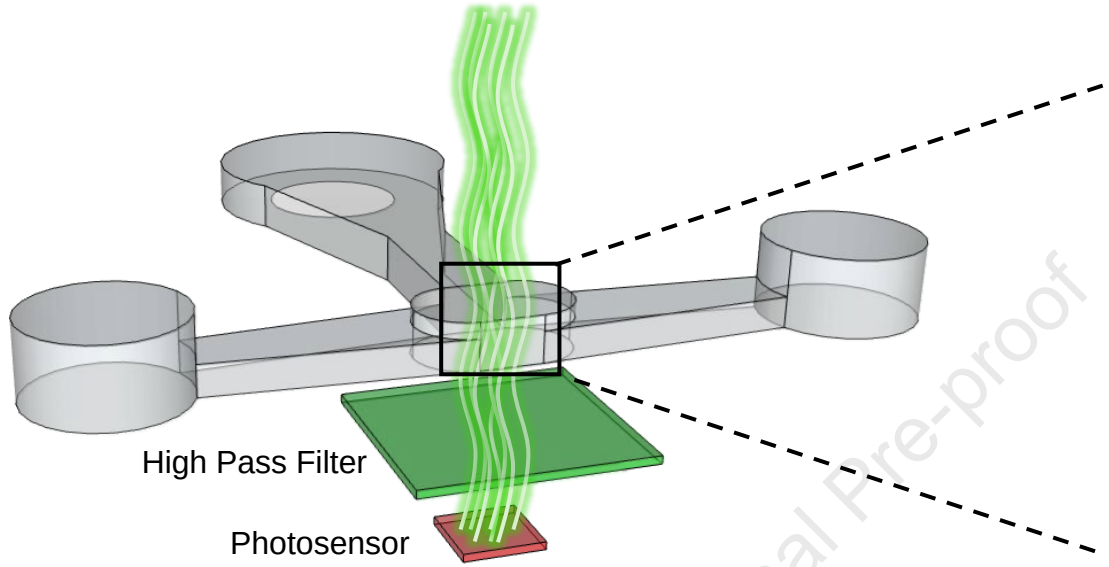

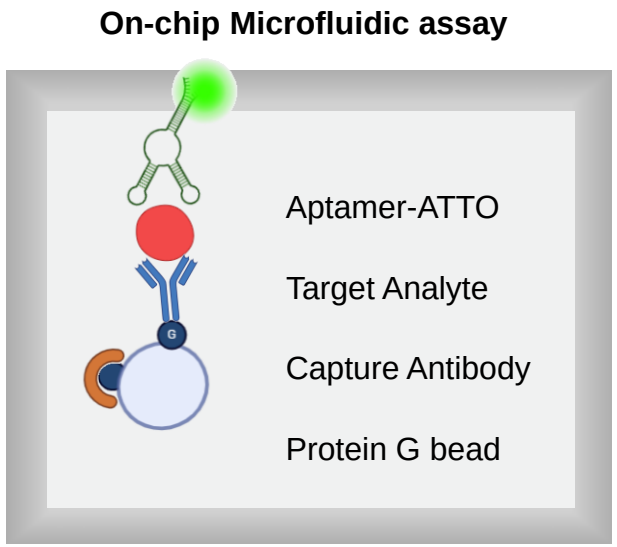

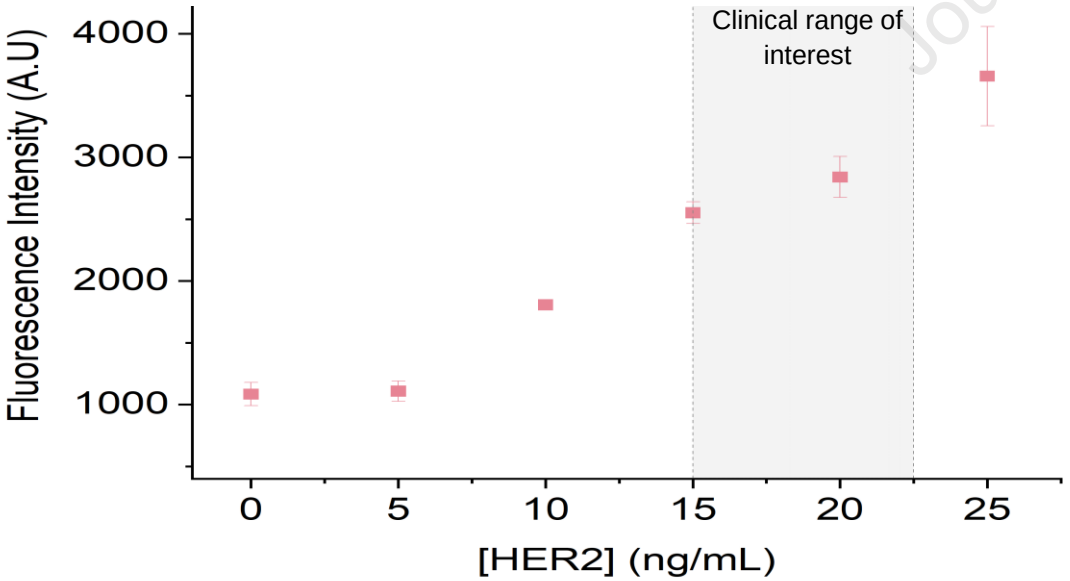

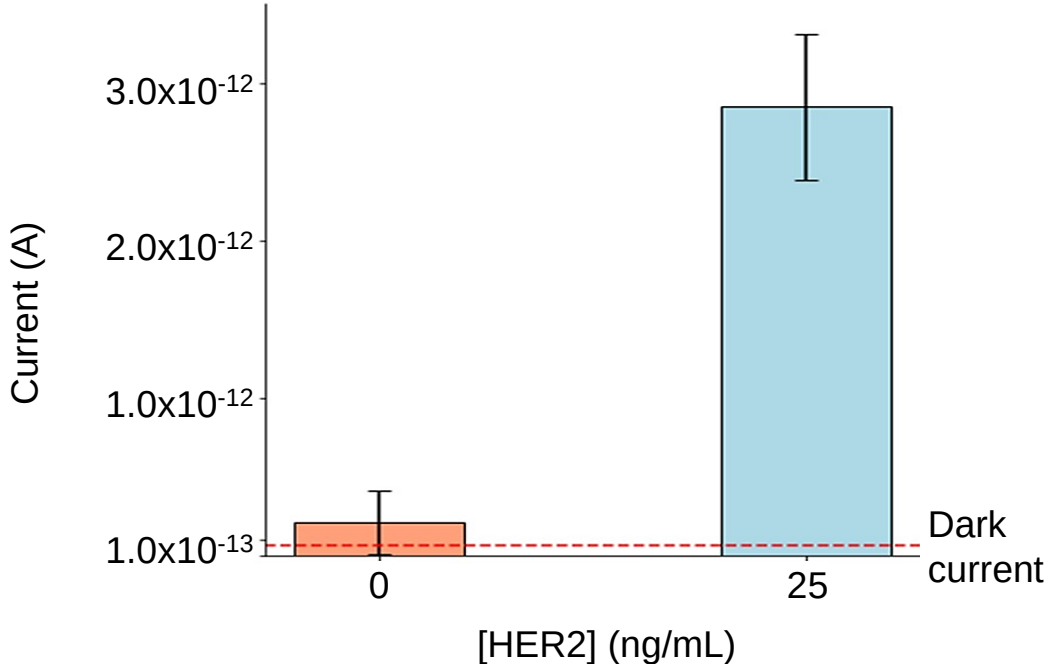

Microfluidic fluorescence biosensor for quantitative detection of HER2 in serum using an antibody–aptamer sandwich assay

J.P. Conde[1,2], M.R.V.C. Pinho[1], M.S.M. Mendes[1,3], I. Agostinho[1], R.G. Rodrigues[1], F.A. e Silva[3], M.G. Freire[3], V. Chu[1]

[1]Instituto de Engenharia de Sistemas e Computadores – Microsistemas e Nanotecnologias (INESC MN), Lisbon, Portugal

[2]Department of Bioengineering, Instituto Superior Técnico, Universidade de Lisboa, Lisbon, Portugal

[3]CICECO – Aveiro Institute of Materials, Department of Chemistry, University of Aveiro, Aveiro, Portugal

Abstract

Early detection of cancer biomarkers requires analytical platforms capable of sensitive quantification in complex biological matrices. Here we report a microfluidic fluorescence biosensor for the quantification of the breast cancer biomarker Human epidermal growth factor receptor 2 in human serum. The system integrates a hybrid bead-based antibody–aptamer sandwich assay with thin-film hydrogenated amorphous silicon (a-Si:H) photodiodes and a dielectric interference filter, enabling compact on-chip fluorescence detection within a fully integrated microfluidic architecture.

Protein G-functionalized microbeads enabled oriented immobilization of capture antibodies, while a fluorophore-labeled HER2 aptamer served as the detection probe, forming a hybrid antibody–aptamer recognition scheme that minimized non-specific interactions in serum matrices. The microfluidic architecture and washing direction were optimized to suppress residual unbound aptamer, significantly improving the signal-to-background ratio.

Under optimized conditions, the biosensor exhibited a near-linear fluorescence response for HER2 concentrations in 90% human serum across clinically relevant levels, achieving a limit of detection of 7–8 ng mL^{-1}, below the clinical threshold of 15 ng mL^{-1}. Photodiode measurements were consistent with fluorescence microscopy, confirming reliable on-chip signal acquisition.

These results demonstrate a scalable strategy that combines hybrid molecular recognition, microfluidic background suppression, and integrated thin-film photodetection within a compact fluorescence biosensing platform for quantitative biomarker analysis.

Keywords:

HER2
Microfluidic biosensor
Aptamer–antibody assay
Fluorescence detection
Serum biomarker analysis

INTRODUCTION

Cancer remains one of the leading causes of mortality worldwide, accounting for approximately one in five deaths globally [1–3]. Early detection significantly improves treatment outcomes, yet diagnosis is often delayed because early-stage disease produces few or non-specific symptoms [4–7]. Screening programs therefore play a crucial role in identifying cancer at earlier stages. In addition to imaging approaches such as mammography, blood-based biomarker detection—commonly referred to as liquid biopsy—offers a minimally invasive and cost-effective alternative for early diagnosis. Analytical platforms capable of detecting biomarkers in complex biological matrices with high sensitivity and reliability are therefore of considerable interest.

Microfluidic technologies provide attractive solutions for such assays by reducing sample and reagent consumption while enabling rapid and automated processing [8–10]. In recent years, microfluidic technologies have emerged as powerful tools for bioanalytical and diagnostic applications due to their ability to precisely manipulate small fluid volumes within miniaturized platforms. Microfluidic systems enable improved mass transport, reduced assay times, low reagent consumption, and the integration of multiple analytical steps within a single device. These features have supported the development of compact biosensing platforms for applications including immunoassays, nucleic acid detection, cell analysis, and point-of-care diagnostics [8-10]. In particular, the integration of microfluidics with optical and electrochemical detection strategies has attracted significant interest for decentralized biomarker analysis.

The protein biomarker Human epidermal growth factor receptor 2 is overexpressed in a significant fraction of breast cancers and has served as an important diagnostic and therapeutic target for more than two decades [11,12]. Accurate quantification of HER2 in serum, particularly near clinically relevant thresholds around 15 ng mL^{-1}, is therefore of high clinical relevance [13]. Currently, HER2 detection is most commonly performed using sandwich enzyme-linked immunosorbent assays (ELISAs), in which a capture antibody binds the target antigen and a labeled secondary antibody generates a measurable signal. While widely used, conventional antibody-based ELISAs suffer from several limitations, including batch-to-batch variability, sensitivity to storage conditions due to protein instability, and non-specific binding that can increase background signals and reduce analytical sensitivity [14,15]. Although numerous biosensing strategies for HER2 detection have been reported, relatively few combine sensitive fluorescence assays with monolithically integrated photodetection in architectures suitable for compact and scalable analytical systems.

Aptamers—single-stranded DNA or RNA oligonucleotides selected through Systematic Evolution of Ligands by Exponential Enrichment—offer an attractive alternative to antibodies as molecular

recognition elements [16–18]. Aptamers can bind their targets with high affinity and specificity while often exhibiting reduced non-specific interactions in complex matrices. In contrast to proteins, nucleic acid aptamers are chemically stable, can refold after thermal denaturation, and allow straightforward chemical modification. Their nucleic acid nature enables convenient functionalization with reporter molecules such as fluorophores, facilitating sensitive optical detection in ELISA-like analytical formats.

In this work, we present an integrated microfluidic fluorescence biosensing platform for the quantification of HER2 in human serum. The system combines protein G-functionalized microbeads for oriented immobilization of capture antibodies with a fluorophore-labeled HER2 aptamer in a hybrid antibody–aptamer sandwich assay, enabling high-affinity recognition while reducing non-specific interactions in complex biological matrices. The microfluidic chamber geometry and washing configuration were optimized to suppress residual unbound fluorescent probes, thereby improving the signal-to-background ratio. Fluorescence detection was implemented using thin-film hydrogenated amorphous silicon (a-Si:H) p–i–n photodiodes integrated with a dielectric interference filter, enabling compact on-chip signal acquisition without bulky external optics. Under optimized conditions, the platform enabled detection of HER2 in 90% human serum with a limit of detection of 7–8 ng mL^{-1}, below the clinically relevant threshold. These results demonstrate a scalable strategy for integrating fluorescence assays with thin-film photodetectors toward compact analytical biosensing systems. The analytical performance of the proposed system is evaluated in terms of sensitivity, limit of detection, dynamic range, and operation in complex serum matrices, demonstrating its suitability for quantitative biomarker analysis. To the best of our knowledge, few reported HER2 biosensing systems combine hybrid antibody–aptamer recognition, optimized microfluidic background suppression, and integrated thin-film fluorescence photodetection within a single analytical platform.

METHODS

Microfabrication

Microfluidic structures

The microfluidic structures were designed with two different heights: 20 µm height connecting channels and a 100 µm height channel/chamber. Figure 1 schematically depicts the configuration and dimensions of the devices used. To create the two-level device, two hard masks were fabricated to make the master mold. For that, 200 nm thick AlSiCu layers were deposited (Nordiko 7000) on glass substrates (Corning Inc, Corning, NY, USA) and patterned by Direct Write Lithography (Heidelberg Instruments, Heidelberg, Germany) and wet etching (TechniEtch A180, Microchemicals, Ulm, Germany). The fabrication of the master mold started with the spin coating (Laurell Technologies Corp., Landale, PA, USA) of SU-8 2015

(Micro Resist Technology, Berlin, Germany) to a thickness of 20 µm on a silicon substrate (University Wafer, South Boston, MA, USA) and UV lithographic patterning (UV KUB-2, KLOÉ, St Mathieu de Tréviers, France) using the hard mask previously fabricated. The process was then repeated for the 100 µm thick layer using SU-8 50 (Micro Resist Technology, Berlin, Germany) on top of the 20 µm layer.

To replicate the negative of the pattern imprinted on the SU-8 mold, polydimethylsiloxane (PDMS) (SYLGARD 184 Silicone Elastomer, Dow Corning, Midland, MI, USA) base and curing agent were thoroughly mixed at a 10:1 weight ratio. The mixture was degassed in a desiccator (Bel-Art Products, Warminster, PA, USA) and cast from the master mold by curing in an oven (Memmert, Schwabach, DE) at 70 °C for 90 minutes. After curing, the PDMS microfluidic layer was peeled from the mold, while inlets and outlets were punched through the PDMS layer using a 20-gauge syringe needle (Instech Laboratories, Plymouth Meeting, PA, USA).

To seal the microfluidic channels, a 500 µm thickness PDMS membrane was spin coated on a silicon wafer with the same 10:1 PDMS mixture and cured at 70 °C for 90 minutes.

Both the microfluidic layer and the membrane were then treated in an O_2 plasma (Harrick Plasma, Ithaca, NY, USA) with 30 W for 1 minute to activate their surfaces by creating hydroxyl groups. Upon bringing the two surfaces together, covalent bonds were established resulting in irreversible sealing.

***p-i-n* a-Si:H photosensor fabrication**

Hydrogenated amorphous silicon (a-Si:H) *p-i-n* photodiodes with active areas of 200 µm × 200 µm were fabricated following an established protocol [19–21]. The process began with Corning 1737 glass substrates, onto which a 200 nm thick AlSiCu bottom contact was deposited by DC magnetron sputtering (Nordiko 7000; 2 kW, 3.0 mTorr, room temperature). This metallization was patterned using 1.4 µm-thick positive photoresist and photolithography (Heidelberg Instruments Direct Write Lithography, Heidelber, Germany), followed by wet etching to define the electrode contacts.

The a-Si:H *p-i-n* multilayer structure was deposited sequentially by radio-frequency plasma-enhanced chemical vapor deposition (rf-PECVD, Oxford Instruments, Bristol, UK) at 300 °C and 350 mTorr, with a rf power of 10 W. The following gas flows were used for each layer: intrinsic a-Si:H (25 sccm SiH_4 and 10 sccm H_2, thickness 5000 Å); n-type a-Si:H (50 sccm SiH_4, 26 sccm H_2, and 30 sccm PH_3, thickness 500 Å); p-type a-Si:H (50 sccm SiH_4 and 50 sccm B_2H_6, thickness 200 Å).

Subsequently, a 50 nm thick indium tin oxide (ITO, resistivity = 500 µΩ·cm) layer was deposited by DC magnetron sputtering (Alcatel) to serve both as the top contact and as a protective layer during subsequent etching. Photolithography and reactive ion etching (RIE; LAM Research Rainbow Plasma Etcher, Fremont, CA, USA) were then used to pattern the *p-i-n* islands.

The sidewalls of the *p-i-n* structures were coated with 200 nm of silicon nitride (SiN_x) using PECVD (Oxford Instruments, Bristol, UK) at 300 °C and 1000 mTorr, with a rf power of 20 W (20 sccm SiH_4, 20 sccm NH_3, and 980 sccm N_2), and electrical vias were opened by photolithography and RIE (LAM Research Rainbow Plasma Etcher, Fremont, CA, USA).

Finally, AlSiCu interconnect lines (200 nm thickness) were defined by a lift-off process, linking the ITO top contacts for external electrical interfacing.

Fluorescence filter fabrication and integration

Optical interference filter stacks were fabricated to match the spectral requirements of the fluorophore used in this work (ATTO series). For fluorescence detection, a high-pass filter was designed to efficiently block excitation light while maximizing transmission of the fluorophore's emission. Given the proximity of the excitation and emission wavelengths, filter design prioritized excitation blocking (elimination) without significantly compromising emission throughput.

The high-pass filter consisted of a Distributed Bragg Reflector (DBR) made from alternating layers of silicon nitride (SiN_x) and silicon dioxide (SiO_2) [20]. This DBR structure was optimized to block the 488 nm excitation wavelength and transmit emission at 505 nm. Both dielectric layers were deposited by radio-frequency plasma-enhanced chemical vapor deposition (rf-PECVD). The details of the fabricated filter layers can be found in Table S1 in the Supplementary Information.

Specifically, the SiN_x layers were deposited at 300 °C, under 1000 mTorr chamber pressure, with applied plasma powers of 20 W (high frequency) and 23 W (low frequency). Gas flows were set to 20 sccm SiH_4, 998 sccm N_2, and 2 sccm NH_3. These conditions were tuned to yield a refractive index of 2.6 at 633 nm, as required by optical filter design. The SiO_2 layers were deposited at 300 °C and 1000 mTorr, with a plasma power of 20 W and gas flows of 161.5 sccm N_2 and 8.5 sccm SiH_4.

The completed optical filters were deposited onto glass substrates and subsequently positioned above the photosensor array. Mechanical alignment was performed under the microscope to ensure correspondence between the photosensors and the microbead chamber within the microfluidic structure.

The filter transmission was evaluated using a picoammeter (Keithley 237, Tektronix, Beaverton, OR, USA) to measure the photodiode current, while being illuminated by a tungsten-halogen lamp (Oriel model 6618, Newport Corp., Irvine, CA, USA) in combination with a monochromator (Oriel model 77250 Series 1/8 m, Newport Corp., Irvine, CA, USA). The measured transmittance of the filter can be found in Figure S1 in the Supplementary Information.

HER2 aptamer-based assay

Reagents and solutions

Protein G Sepharose® 4 Fast Flow beads (17-0618-01) were acquired from Cytiva (Marlborough, MA, USA). Phosphate buffered saline (PBS) 10x (BP3991) was acquired from Thermo Fisher Scientific (Waltham, MA, USA). TE buffer 1x (12090015) and goat anti-human immunoglobulin G (IgG, 1 mg/mL) (A18812) were obtained from Invitrogen (Carlsbad, CA, USA). Human serum (H4522) was obtained from Sigma Aldrich (St. Louis, MO, USA), while both the capture antibody anti-HER2 (1.009 mg/mL) (ab281274-1001) and HER2 protein (ab168896) were purchased from Abcam (Cambridge, UK). The recombinant protein was reconstituted in deionized water and diluted to final working solutions composed of 90% human serum ranging from 0 to 100 ng/mL of HER2.

HER2 aptamer conjugated with ATTO was reconstituted in TE buffer to a concentration of 100 µM (HER2 Aptamer Sequence /5 ATTO430 LN/ AA CCG CCC AAA TCC CTA AGA GTC TGC ACT TGT CAT TTT GTA TAT GTA TTT GGT TTT TGG CTC TCA CAG ACA CAC TAC ACA CGC ACA, conjugated with ATTO, Non-Catalog Synthesis Request from Integrated DNA Technologies – IDT (Coralville, IO, USA). This sequence was obtained from ref. [22], in which this sequence was found to bind to an epitope peptide of HER2 and to the extracellular domain of the HER2 protein, with minimal cross reactivity to albumin or trypsin. The aptamer was also found to preferentially bind to HER2-positive but not HER2-negative breast cancer cells [22]. To acquire an optimal configuration, the aptamers were heated at 95 °C for 5 minutes followed by 1 minute cooldown in ice.

Fluidic handling

Fluid flow in the microfluidic structures was controlled using a syringe pump NE-1002X (New Era Pump Systems, Farmingdale, USA), operated in pulling mode, and connected at the outlet. The pump was equipped with a 1 mL syringe filled with PBS, which was linked to the microfluidic outlet via a polyethylene tube and a stainless-steel tube adapter.

The solutions to be introduced were loaded into standard micropipette tips, which were manually inserted into the PDMS inlets. Upon pump activation, negative pressure was applied at the outlet, drawing the solution through the microchannels from the inlet reservoir.

Figure 1 shows a schematic of the microfluidic chamber. Prior to biosensing experiments, the microfluidic structure was packed with microbeads to form the sensing bed [23-24]. Initially, PBS 1x was flowed through the channel at 8 µL/min as cleaning step and 20 µL of microbeads were loaded into a micropipette tip inserted at the bead packing inlet. The negative pressure applied at the outlet by the syringe pump at a flow rate of 8 µL/min resulted in the beads being driven either into the bead chamber (Figure 1a)) or the microfluidic channel (Figure 1b)).

Due to their diameter range of 40–90 µm, the beads were confined within the bead chamber, restricted from entering the microchannels by its height of 20 µm height. After bead loading, a final PBS wash was

performed at 8 µL/min to compact the beads.

Contrary to the linear structure (Figure 1b)), the chamber structure (Figure 1a)) was designed with different packing and reagents inflow inlets. Once the bead chamber was packed and washed, the bead packing inlet, in the chamber structure, was sealed with a 20-gauge closed metal plug.

Multiple inlet and outlet configurations were tested throughout the experiments to accommodate different assay conditions, as illustrated in Figure S2 in the Supplementary Information. All biosensing assays followed a standardized flow protocol consisting of reagent flow at 0.5 µL/min for 10 minutes and intermittent washes with PBS 1x in between steps at 5 µL/min for 1 minute. The sequential reagent solutions were applied in the following order: capture antibody (100 µg/mL), blocking agent (1 mg/mL IgG), HER2 in PBS 1x or 90% human serum, and labelled aptamer (5 µM). The washing step at the end varied according to the specific conditions tested. For the chamber structure (Figure 1a)), two different washing configurations were tested: reagent wash in which PBS 1x was flowed from the reagent inlet to the outlet (Figure S2b)) and packing wash in which PBS 1x flowed from the bead packing inlet to the outlet (Figure S2c)).

Measurements and data analysis

Fluorescence measurements with microscope

Fluorescence measurements were performed using a fluorescence microscope (LEICA DMLM, Wetzlar, Germany) equipped with digital camera (DFC300FX) and a CoolLED lamp (pE-300lite) as light source, and an I3 filter cube for excitation in 450-490 nm correspondent to blue region.

ImageJ software from the National Institute of Health, USA, was used to analyze fluorescence data. The assay fluorescence signal was obtained by subtracting the background signal acquired from the area outside of the microfluidic structure from the signal acquired from the inner chamber area. All fluorescence images were acquired under 10x magnification, 1x gain, and using an exposure time of 2 s.

Fluorescence measurements with a-Si:H photodiodes

The a-Si:H photodiodes were wire-bonded to a custom PCB and then connected to a picoammeter (Keithley 237, Tektronix, Beaverton, OR, USA) to acquire the photocurrent. During the fluorescent measurements, light from a 405 nm excitation laser was focused on the photodiode at normal incidence through the microfluidic chamber. Fig. S4 shows a typical dark I-V and photocurrent as a function of photon flux for the microfabricated a-Si:H photodiodes.

RESULTS AND DISCUSSION

Integrated biosensing platform architecture

The developed platform integrates microfluidic sample handling, bead-based bio-recognition, optical filtering, and thin-film photodetection within a vertically stacked architecture designed for compact fluorescence biosensing. Fig. 2 presents a schematic of this platform.

The microfluidic structure incorporates a bead-retention chamber with defined height transitions that confine protein G-functionalized microspheres while enabling controlled reagent delivery and washing. This geometry was intentionally designed to maximize probe density and minimize diffusion distances while preserving compatibility with underlying photodiode alignment.

Protein G-functionalized microbeads were selected to promote oriented immobilization of anti-HER2 capture antibodies, increasing effective binding site availability and enhancing assay sensitivity. Detection was achieved using a fluorophore-labeled HER2 aptamer, forming a hybrid antibody–aptamer sandwich configuration that combines the robustness of antibody capture with the reduced non-specific adsorption typically associated with nucleic acid probes. The complete assay sequence—capture, blocking, target binding, and fluorescent aptamer labeling—was implemented under continuous flow conditions within the microfluidic chamber. Fig. 2 presents also a summarized schematic of the detection assay.

Because fluorescence detection is performed using an integrated thin-film photodiode positioned beneath the microfluidic chamber, the fluidic architecture and washing strategy were optimized to minimize residual unbound fluorescent probes that could otherwise contribute to background signal. This co-design of assay chemistry, microfluidics, and photodetection enables compact fluorescence biosensing without reliance on external microscopy.

Assay optimization and background suppression strategy

Microbeads functionalized with protein G were used to immobilize the capture antibodies (anti-HER2) due to their high surface area for probe molecule attachment and reduced diffusion distances for both target and detection molecules. These properties collectively enhance assay sensitivity by increasing the overall transduction signal. The microbeads were introduced into the microfluidic device through the packing inlet and subsequently trapped in the bead chamber. Figure 1 depicts schematically the microfluidic chambers used, highlighting the different heights of the various sections. The retention is achieved by a height difference between the bead chamber and both the reagent inlet and outlet channels, as illustrated in Figure 1a).

The overall assay strategy is shown in Figure 3. Initially, the capture antibodies are immobilized onto the microbeads via specific binding to the protein G at the surface (Figure 3a)). Following antibody immobilization, the bead surface is passivated to minimize non-specific interactions (Figure 3b)).

Subsequently, the target analyte is introduced and will specifically bind to the immobilized capture antibodies (Figure 3c)). Finally, a detection probe, consisting of a fluorophore-labeled aptamer, binds to the captured target analyte, thus completing the sandwich assay format (Figure 3d)). Each step is separated by an intermediate washing step with PBS to remove unbound material. Notably, employing an aptamer as the detection probe is advantageous for reducing non-specific binding to the protein G-functionalized beads, thereby improving assay specificity.

Key assay parameters, including the optimal concentration of HER2 aptamer (5 µM), the most effective blocking solution (1 mg/mL IgG), and the appropriate aptamer buffer (TE buffer) [data not shown] were optimized. In addition, sample preparation protocols were evaluated by comparing the fluorescence intensity ratios obtained in the presence of 0 and 25 ng/mL of target analyte, both in PBS and human serum. These studies show that the post-aptamer incubation washing step (specifically, the choice of flow rate, duration, washing buffer, and inlet selection) is critical for minimizing assay variability and reducing non-specific signal contributions. As a result, the optimization of the final wash parameters became a central focus in further assay development.

To investigate the source of variability in fluorescence intensity, the signal was monitored multiple times during the final wash rather than relying solely on endpoint measurements. Time-resolved fluorescence monitoring during the final wash revealed accumulation of labeled aptamer near the lower region of the bead chamber, close to the packing inlet, as illustrated in Figure S3. This residual probe contributed significantly to background signal under the standard washing configuration. Under the standard washing procedure, where the wash buffer was introduced through the reagent inlet channel, the aptamer was only slowly eluted from this region resulting in significant fluorescence signal even with 0 ng/mL of HER2. To address this limitation, the flow configuration of the microfluidic structure was modified. Following the completion of aptamer flow, the reagent inlet was plugged, and the final wash buffer was introduced through the bead packing inlet instead. This altered protocol significantly improved the efficiency of removing unbound labeled aptamer, thereby reducing fluorescence variability and enhancing assay performance. Optimal results were achieved with a final wash at 2.5 µL/min for 5 minutes via the packing inlet, which efficiently eliminated non-specific signal from excess suspended aptamer (Figure 4a)). This protocol maintained a high fluorescence signal ratio between 0 and 25 ng/mL analyte concentrations in both PBS and 90% human serum, as shown in Figure 4b), where fluorescence was measured within the bead chamber.

Analytical performance in serum

Finally, the analytical validity of the assay for detection of HER2 in human serum was assessed in terms of its sensitivity and applicability in a clinical range of interest. This was achieved through a calibration

curve of fluorescence intensity signal obtained for various discrete concentrations of HER2 in 90% human serum (diluted in PBS). Figure 5 presents the HER2 sensitivity curve obtained under the optimized washing conditions in 90% human serum. The fluorescence intensity exhibited an approximately linear relationship with HER2 concentration across the tested range, which encompasses clinically relevant values highlighted by a shaded region in Figure 5. Importantly, the assay distinguished HER2 concentrations within the clinically relevant range, including the established breast cancer testing threshold of 15 ng/mL. The limit of detection (LOD), calculated as three times the standard deviation of the blank, was estimated to be 7–8 ng/mL, demonstrating clinically relevant sensitivity. The limits of detection (LODs) were calculated as the mean value of the blank sample (control sample with 0 ng/mL HER2) plus three times the standard deviation of the blank signal. A linear response was observed above 5 ng/mL of HER2. Note that concentrations above 25 ng/ml of HER2 were not tested as they are significantly above the clinically relevant range.

The use of 90% human serum as the assay matrix provides a biologically relevant environment that simulates the complexity of clinical samples, including non-specific adsorption and matrix-associated background effects.

Integrated thin-film photodiode validation for on-chip fluorescence detection

To demonstrate compact fluorescence readout without reliance on external microscopy, the optimized assay was implemented using an integrated thin-film hydrogenated amorphous silicon (a-Si:H) p–i–n photodiode manually aligned beneath the microbead chamber. A dielectric multilayer high-pass interference filter was positioned between the microfluidic structure and the photodiode to suppress excitation leakage while transmitting the fluorophore emission band, thereby minimizing optical cross-talk and enhancing signal-to-background ratio.

The integrated configuration is schematically illustrated in Fig. 2 and in more detail in Fig. 6, showing vertical alignment of the bead chamber, interference filter, and photodiode active area. This stacked architecture enables direct fluorescence collection from the sensing region while maintaining a compact footprint compatible with scalable thin-film fabrication. The thin-film nature of the a-Si:H photodiodes enables monolithic integration with microfluidic substrates and multiplexed sensor arrays, providing a pathway toward simultaneous detection of multiple biomarkers within a single compact platform. The linear sensor array architecture is inherently compatible with spatial multiplexing, enabling future detection of multiple biomarkers within a single microfluidic platform.

Photocurrent measurements were acquired under excitation illumination for HER2 concentrations of 0 and 25 ng/mL in 90% human serum. At 0 ng/mL, the measured signal was indistinguishable from the photodiode dark current within experimental uncertainty, indicating effective suppression of

background fluorescence through the combined effects of directional washing and optical filtering. In contrast, at 25 ng/mL HER2, a clear and reproducible increase in photocurrent relative to the blank measurement was observed, demonstrating reliable transduction of the fluorescence signal by the thin-film sensor (Figure 5c). The photodiode dark current was 10^{-13} A ($\sim 10^{-10}$ A.cm^{-2}) with noise equivalent power (NEP) of ~6×10^{-14} W and specific detectivity (D*) of ~10^{11} Jones [19].

Importantly, the relative signal increase measured with the integrated photodiode was consistent with the fluorescence intensity trends obtained by epifluorescence microscopy at the corresponding HER2 concentrations. Although only representative concentrations (0 and 25 ng mL^{-1}) were evaluated using the integrated detector, this agreement supports the feasibility of the on-chip fluorescence readout and confirms that miniaturized photodetection preserves the analytical behavior observed with conventional optical characterization. These findings are also consistent with previous studies employing thin-film photodiodes for integrated fluorescence biosensing [25-27]. The ability to resolve clinically relevant HER2 concentrations using a thin-film photodiode platform highlights the compatibility of fluorescence-based bioassays with scalable semiconductor fabrication processes.

These results validate the co-design strategy adopted in this work, in which microfluidic washing architecture, optical filtering, and photodiode positioning were jointly optimized to achieve low-background fluorescence sensing. The integrated detection module thus represents a key step toward compact, multiplexable fluorescence biosensors for point-of-care biomarker monitoring.

The present platform was developed as a proof-of-concept integrated biosensing system using PDMS-based microfluidics to facilitate rapid prototyping and iterative optimization of assay and flow conditions. Although PDMS is well suited for research-stage device development, the proposed microfluidic architecture is compatible with scalable fabrication approaches based on thermoplastic materials and replication techniques such as injection molding or hot embossing. Importantly, the thin-film a-Si:H photodiodes employed here are inherently compatible with large-area semiconductor manufacturing processes. While additional components required for fully autonomous sample-to-answer operation, including fluid actuation, control electronics, and compact excitation sources, remain to be integrated, the demonstrated architecture provides a viable framework for future miniaturized and potentially portable fluorescence biosensing systems.

The present platform was operated as a single-use microfluidic biosensor. For analytical applications involving complex biological samples such as serum, disposable operation is advantageous for minimizing cross-contamination and carry-over effects between measurements. Furthermore, regeneration of the sensing surface would require removal of bound analyte and fluorescent probes while maintaining the activity of immobilized antibodies and aptamers, which represents a non-trivial

optimization challenge. Although reusable operation may be explored in future studies, disposable implementation remains compatible with low-volume microfluidic operation and scalable fabrication strategies. Disposable biosensor operation is also consistent with current trends in point-of-care diagnostic cartridges and microfluidic bioanalytical systems.

Comparison with state-of-the-art HER2 biosensors

Numerous HER2 biosensing strategies have been reported, encompassing electrochemical, optical, plasmonic, and fluorescence-based platforms (Table 1). Electrochemical aptasensors frequently achieve very low limits of detection through nanomaterial-enhanced signal amplification; however, they typically rely on external potentiostats or dedicated electrochemical workstations for signal acquisition [25–27]. Optical approaches, including surface plasmon resonance (SPR), provide label-free detection with high sensitivity but generally depend on benchtop optical instrumentation that limits device miniaturization [28]. Similarly, fluorescence-based assays commonly employ microscopy or external photodetectors for readout, restricting integration within compact architectures [29,30].

In contrast, the platform presented here integrates bead-based antibody–aptamer recognition, microfluidic handling, optical filtering, and thin-film a-Si:H photodiode detection within a vertically stacked architecture. This configuration enables direct on-chip fluorescence acquisition without external optical modules while maintaining analytical performance in 90% human serum.

Although some reported biosensors achieve lower detection limits under optimized buffer conditions, the present system provides clinically relevant sensitivity while enabling direct fluorescence readout using integrated thin-film photodiodes within a compact microfluidic architecture. While the present work demonstrates clinically relevant sensitivity, further improvements in signal amplification and background suppression could extend detection to lower concentration regimes. Importantly, this sensitivity is realized within a compact and potentially scalable device architecture. The co-optimization of microfluidic flow configuration, background suppression through washing control, optical filtering, and photodiode alignment highlights a system-level engineering approach that extends beyond assay development toward integrated biosensor design. Although the total assay time remains comparable to other fluorescence-based biosensing strategies, future optimization of incubation and washing steps may further reduce analysis time.

Although a detailed economic analysis is beyond the scope of the present proof-of-concept study, several aspects of the proposed platform are compatible with cost reduction and scalable manufacturing. The microfluidic format minimizes reagent and sample consumption, while the use of thin-film a-Si:H photodiodes enables fabrication using scalable semiconductor deposition processes over large areas. In addition, integrated fluorescence detection eliminates the need for bulky and costly microscopy-based

instrumentation. The use of aptamer probes may also contribute to reduced assay costs and improved storage stability compared with fully antibody-based systems. Collectively, these features are a step toward scalable fluorescence biosensing platforms that couple molecular specificity with thin-film semiconductor photodetection for miniaturized biomarker analysis. Furthermore, these features support the potential development of compact and cost-effective biosensing platforms for decentralized biomarker analysis. Table S2 summarizes these qualitative cost considerations of the proposed biosensing platform.

CONCLUSIONS

A central innovation of this work is the co-design of molecular recognition chemistry, microfluidic washing architecture, and thin-film photodetector integration to enable low-background fluorescence sensing within a compact analytical platform.

In this work, a fluorescence-based aptamer assay for the detection of the HER2 protein was developed and implemented within a microfluidic sensing platform. The system combines the high specificity of a HER2-targeting aptamer with fluorescence signal modulation, enabling sensitive detection of the target protein within a defined analytical range and with a low limit of detection. The assay also demonstrates good selectivity toward HER2 in the presence of non-target proteins.

Integration of the sensing strategy into a microfluidic format enables controlled handling of small sample volumes and provides a convenient platform for performing the assay under well-defined conditions. This integrated approach highlights the potential of combining aptamer-based molecular recognition with microfluidic technologies to develop compact and efficient analytical systems for protein detection.

Although the present study demonstrates analytical performance in complex serum matrices, future work will focus on validation using clinically derived patient samples and larger cohorts to further assess the translational potential of the platform.

Overall, the proposed platform represents a promising strategy for HER2 sensing and illustrates the potential of integrated microfluidic–fluorescence approaches for biomarker analysis. Although further engineering integration will be required for fully autonomous point-of-care implementation, the demonstrated architecture is compatible with scalable microfluidic and thin-film semiconductor fabrication strategies. The demonstrated integration of hybrid antibody–aptamer recognition, engineered microfluidic handling, and thin-film fluorescence detection provides a scalable framework for compact and potentially multiplexed biomarker sensing platforms.

Acknowledgements

The authors thank Peter Gohl for helping with the measurements using the photodetectors. This work was supported by Fundação para a Ciência e a Tecnologia (FCT) by funding the research project ILSurvive (PTDC/EMD-TLM/3253/2020; DOI: 10.54499/PTDC/EMD-TLM/3253/2020) and project MIDIFRUIT (DOI: 10.54499/2023.16677.ICDT), and the Research Unit INESC MN (UID/05367/2020) through Pluriannual financing (UIDB/05367/2025, UID/PRR/5367/2025 and UID/PRR2/05367/2025). This work was also developed within the scope of the project CICECO – Aveiro Institute of Materials, UIDB/50011/2020 (DOI: 10.54499/UIDB/50011/2020), UIDP/50011/2020, (DOI: 10.54499/UIDP/50011/2020) and LA/P/0006/2020 (DOI: 10.54499/LA/P/0006/2020), financed by national funds through the FCT/MEC (PIDDAC). The authors also thank FCT for the doctoral grants of R.G. Rodrigues (2022.14483.BD) and M.S.M. Mendes (2022.11229.BD; DOI 10.54499/2022.11229.BD). F.A. e Silva acknowledges FCT for the researcher contract CEECIND/03076/2018/CP1559/CT0024 (DOI: 10.54499/CEECIND/03076/2018/CP1559/CT0024) under the Scientific Employment Stimulus – Individual Call 2018).

References

[1] OECD. 2023. *Country Health Profile 2023: Portugal*. OECD Publishing, Paris. https://doi.org/10.1787/2e35af61-en

[2] J. Ferlay, M. Ervik, F. Lam, et al., "*Global Cancer Observatory: Cancer Today"*. Lyon, France: International Agency for Research on Cancer. 2020. https://gco.iarc.fr/today

[3] Bray F, et al. Global cancer statistics 2018: GLOBOCAN estimates of incidence and mortality worldwide for 36 cancers in 185 countries. *CA Cancer J Clin*. 2018;68(6):394-424. https://doi.org/10.3322/caac.21492

[4] W. Ren, M. Chen, Y. Qiao, and F. Zhao, "Global guidelines for breast cancer screening: A systematic review", Breast 64, 85-99 (2022). https://doi.org/10.1016/j.breast.2022.024.003

[5] A. M. Lennon, A. H. Buchanan, I. Kinde, et al., "Feasibility of blood testing combined with pet-ct to screen for cancer and guide intervention" Science, 369, 7 (2020). https://doi.org/10.1126/SCIENCE.ABB9601

[6] M. Heidari , et al., "Early Cancer Detection: An Effective Approach for Cancer Control", Asian Pac J Cancer Prev. 21,1519-1525 (2020). https://doi.org/10.31557/APJCP.2020.21.6.1519

[7] R. D. Neal, P. Tharmanathan, B. France, et al., "Is increased time to diagnosis and treatment in symptomatic cancer associated with poorer outcomes, systematic review# Br J Cancer 112, S92-107 (2015). https://doi.org/10.1038/bjc.2015.48.

[8] J.G. Lohr, et al., "Liquid biopsy in cancer detection and monitoring", Nat Rev Clin Oncol. 18, 175-179 (2021). https://doi.org/10.1038/s41571-020-00428-x

[9] L.Y. Yeo, et al., "Microfluidics for Rapid Disease Diagnostics and Near-Patient Testing", Front Bioeng Biotechnol. 9, 606164 (2021). https://doi.org/10.3389/fbioe.2021.606164

[10] A. Alvandi, et al., "Microfluidic technologies for cancer liquid biopsy: Single cell analysis and beyond", Biosens Bioelectron. 185, 113252 (2021). https://doi.org/10.1016/j.bios.2021.113252

[11] C. Gutierrez and R. Schiff, “Her2: biology, detection, and clinical implications”, Archives of pathology & laboratory medicine 135, 55–62 (2011). https://doi.org/10.5858/2010-0454-RAR.1

[12] A.C. Wolff et al., “ Human Epidermal Growth Factor Receptor 2 Testing in Breast Cancer: ASCO/CAP Clinical Practice Guideline Focused Update”, J Clin Oncol. 36, 2105-2122 (2018). https://doi.org/10.1200/JCO.2018.38.1344

[13] A. Shamshirian, A. R. Aref, G. W. Yip, M. Ebrahimi Warkiani, K. Heydari, S. Razavi Bazaz, Z. Hamzehgardeshi, D. Shamshirian, M. Moosazadeh, and R. Alizadeh-Navaei, “Diagnostic value of serum her2 levels in breast cancer: a systematic review and meta-analysis”, BMC cancer 20, 1–10 (2020). https://doi.org/10.1186/s12885-020-07545-2

[14] J R. Crowther, “The ELISA guidebook”, Methods Mol Biol. 149, 1-413 (2001). https://doi.org/10.1385/1-59259-192-2

[15] S.J. Fuller, et al., “Challenges and limitations in antibody-based assays”, Methods Mol Biol.1200, 75-90 (2014).

[16] S. Y. Toh, M. Citartan, S. C. Gopinath, and T. H. Tang, “Aptamers as a replacement for antibodies in enzyme-linked immunosorbent assay”, Biosensors and Bioelectronics 64, 392–403 (2015). ISSN 0956-5663. https://doi.org/10.1016/J.BIOS.2014.09.026.

[17] S. Song, et al., “Aptamer-based biosensors”, TrAC Trends Anal Chem. 27, 108-117 (2008). https://doi.org/10.1016/j.trac.2007.12.004

[18] J. Zhou, J. Rossi, “Aptamers as targeted therapeutics: current potential and challenges”, Nat Rev Drug Discov. 16, 181-202 (2017). https://doi.org/10.1038/nrd.2016.199

[19] D.R. Santos, R.R.G. Soares, V. Chu, J.P. Conde, “Performance of hydrogenated amorphous silicon thin film photosensors at ultra-low light levels: towars attomolar sensitivity in lab-o-chip biosensing applications”, IEEE Sensors Journal 17, 6895-6903 (2017). https://doi.org/10.1109/JSEN.2017.2751253

[20] A.C. Pimentel, D.M.F. Prazeres, V. Chu, J.P. Conde, “Fluorescence detection of DNA using an amorphous silicon p-i-n photodiode”, J. Appl. Phys. 104, 054913 (2008). https://doi.org/10.1063/1.2976343)

[21] K. Nikolaidou, P.G.M. Condelipes, C.R.F. Caneira, M. Krack, P.M. Fontes, H.M. Oliveira, M. Kovačič, J. Krč, M. Topič, S. Cardoso, P.P. Freitas, V. Chu, J.P. Conde, “Monolithically integrated optical interference and absorption filters on thin film amorphous silicon photosensors for biological

detection", Sensors & Actuators B: Chemical 356, 131330 (2022). https://doi.org/10.1016/j.snb.2021.131330

[22] Z. Liu, J.-H. Duan, Y.-M. Song, J. Ma, F.-D. Wang, X. Lu, and X.-D. Yang. Novel her2 aptamer selectively delivers cytotoxic drug to her2-positive breast cancer cells in vitro, Journal of translational medicine 10:1–10, 2012. https://doi.org/10.1186/1479-5876-10-148

[23] I.F. Pinto, R.R.G. Soares, S.A.S.L Rosa, M.R. Aires-Barros, V. Chu, J.P. Conde, A.M. Azevedo, "High-throughput nanoliter-scale analysis and optimization of multimodal chromatography for the capture of monoclonal antibodies", Anal. Chem. 88, 7959-7967 (2016). https://doi.org/10.1021/acs.analchem.6b00781

[24] I.F. Pinto, C.R.F. Caneira, R.R.G. Soares, N. Madaboosi, M.R. Aires-Barros, J.P. Conde, A.M. Azevedo, V. Chu, "The application of microbeads to microfluidic systems for enhanced detection and purification of biomolecules", Methods 116, 112-124 (2017). https://doi.org/10.1016/j.ymeth.2016.12.005

[25] R.R.G. Soares, F. Neumann, C.R.F. Caneira, N. Madaboosi, S. Ciftci, I. Hernández-Neuta, I.F. Pinto, D.R. Santos, V. Chu, A. Russom, J.P. Conde, M. Nilsson, "Silica bead-based microfluidic device with integrated photodiodes for the rapid capture and detection of rolling circle amplification products in the femtomolar range", Biosensors and Bioelectronics 128, 68-75 (2019). (https://doi.org/10.1016/j.bios.2018.12.004)

[26] R.R.G. Soares, D.R. Santos, I.F. Pinto, A.M. Azevedo, M.R. Aires-Barros, V. Chu, J.P. Conde, "Multiplexed microfluidic fluorescence immunoassay with photodiode array signal acquisition for sub-minute and point-of-need detection of mycotoxins", Lab on a Chip 18, 1569-1580 (2018). (https://doi.org/10.1039/C8LC00259B)

[27] P. Novo, G. Moulas, D.M.F. Prazeres, V. Chu, J. P. Conde, "Detection of ochratoxin A in wine and beer by chemiluminescence-based ELISA in microfluidics with integrated photodiodes", Sensors and Actuators B: Chemical 176, 232-240 (2013). (http://dx.doi.org/10.1016/j.snb.2012.10.038)

[28] T. Harahsheh, Y.F. Makableh, I. Rawashdeh, M. Al-Fandi, "Enhanced aptasensor performance for targeted HER2 breast cancer detection by using screen-printed electrodes modified with Au nanoparticles" Biomed Microdevices 23, 46 (2021). https://doi.org/10.1007/s10544-021-00586-9. PMID: 34546397

[29] Y. Zhang, Y. Xu, N. Li, N. Qi, L. Peng, M. Yang, C. Hou, D. Huo, "An ultrasensitive dual-signal ratio electrochemical aptamer biosensor for the detection of HER2", Colloids Surf B Biointerfaces 222, 113118 (2023). https://doi.org/10.1016/j.colsurfb.2022.113118

[30] G. Bezerra, C. Córdula, D. Campos, G. Nascimento, N. Oliveira, M.A. Seabra, V. Visani, S. Lucas, I. Lopes, J. Santos, F. Xavier Jr, M.A. Borba, D. Martins, J. Lima-Filho, “Electrochemical aptasensor for the detection of HER2 in human serum to assist in the diagnosis of early stage breast cancer”, Anal Bioanal Chem. 411, 6667-6676 (2019). https://doi.org/10.1007/s00216-019-02040-5

[31] M. Lobry, M. Loyez, K. Chah, E.M. Hassan, E. Goormaghtigh, M.C. DeRosa, R. Wattiez, C. Caucheteur, “HER2 biosensing through SPR-envelope tracking in plasmonic optical fiber gratings”, Biomed Opt Express. 4, 4862-4871 (2020). https://doi.org/10.1364/BOE.401200

[32] N. Li, Y. Zhang, Y. Xu, X. Liu, Z. Yang, Q. Wang, M. Yang, C. Hou, D. Huo, “An ultra-sensitive fluorescent Aptamer sensor based on 2D MOF for detection of HER2 in serum”, Microchemical Journal 195, 109426 (2023). https://doi.org/10.1016/j.microc.2023.109426

[33] S.Y. Digehsaraei, M. Salouti, B. Amini, S. Mahmazi, M. Kalantari, A. Kazemizadeh, J. Mehrvand, “Developing a fluorescence immunosensor for detection of HER2-positive breast cancer based on graphene and magnetic nanoparticles”, Microchemical Journal 167, 106300 (2021). https://doi.org/10.1016/j.microc.2021.106300

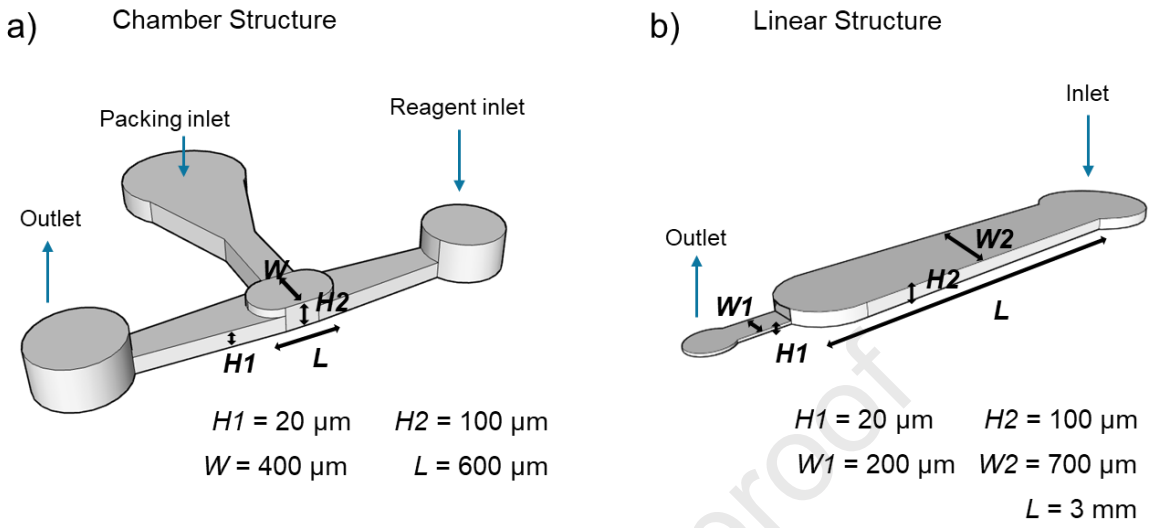

Figure 1 – Microfluidic structures. a) Chamber structure. This structure was used for all experiments except for the one referred to as "linear structure". b) Linear Structure.

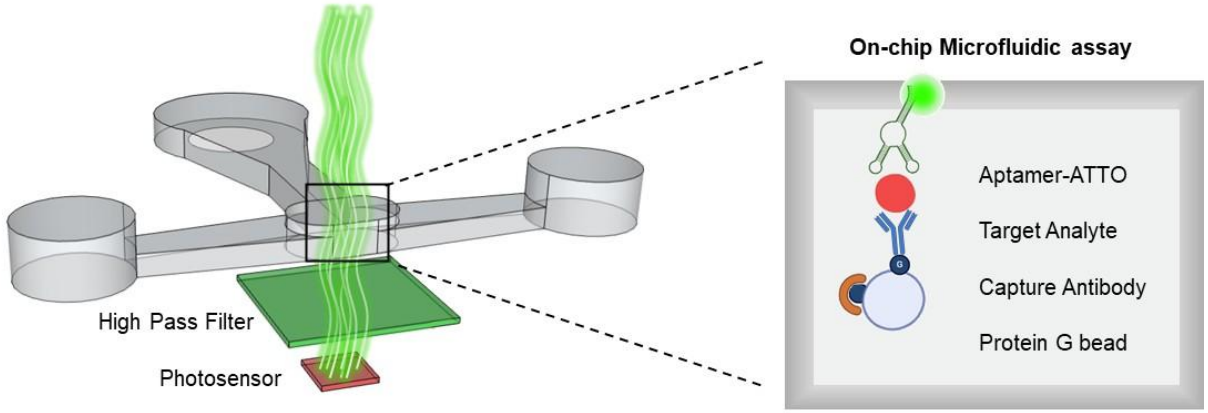

Figure 2 – Schematic representation of the integrated microfluidic network with the microbead chamber aligned to the microfabricated a-Si:H photodetector with an intercalated optical filter to the suppress the excitation light reaching the photodetector (left). On the right, a summary of the analyte (HER2) detection strategy, which involves a capture antibody and a fluorescently labelled anti-target aptamer.

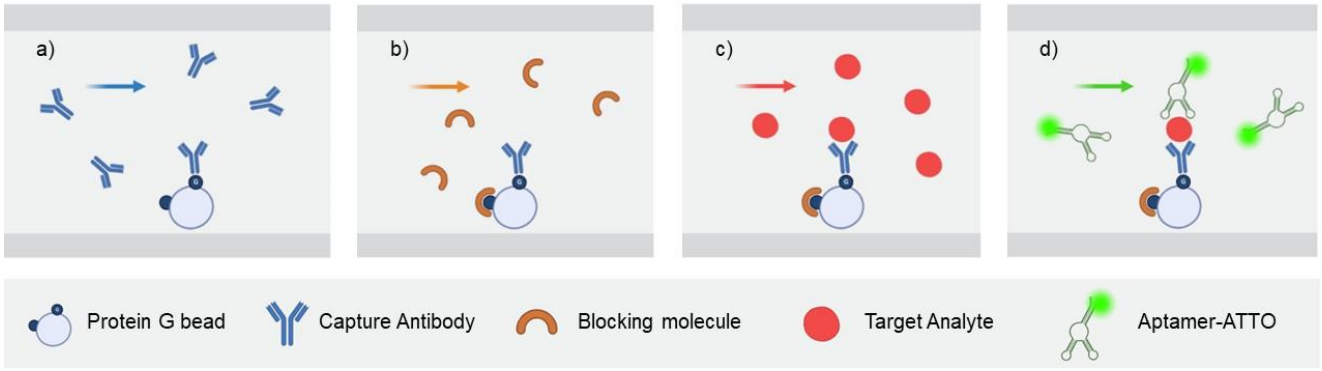

Figure 3 – Bead-based sandwich assay for HER2 detection, comprising the following steps: a) immobilization of anti-HER2 capture antibodies on protein G beads; b) blocking of the bead surface with IgG; c) specific capture of HER2 by the anti-HER2 antibodies; and d) detection of the captured HER2 using ATTO-labelled anti-HER2 aptamers.

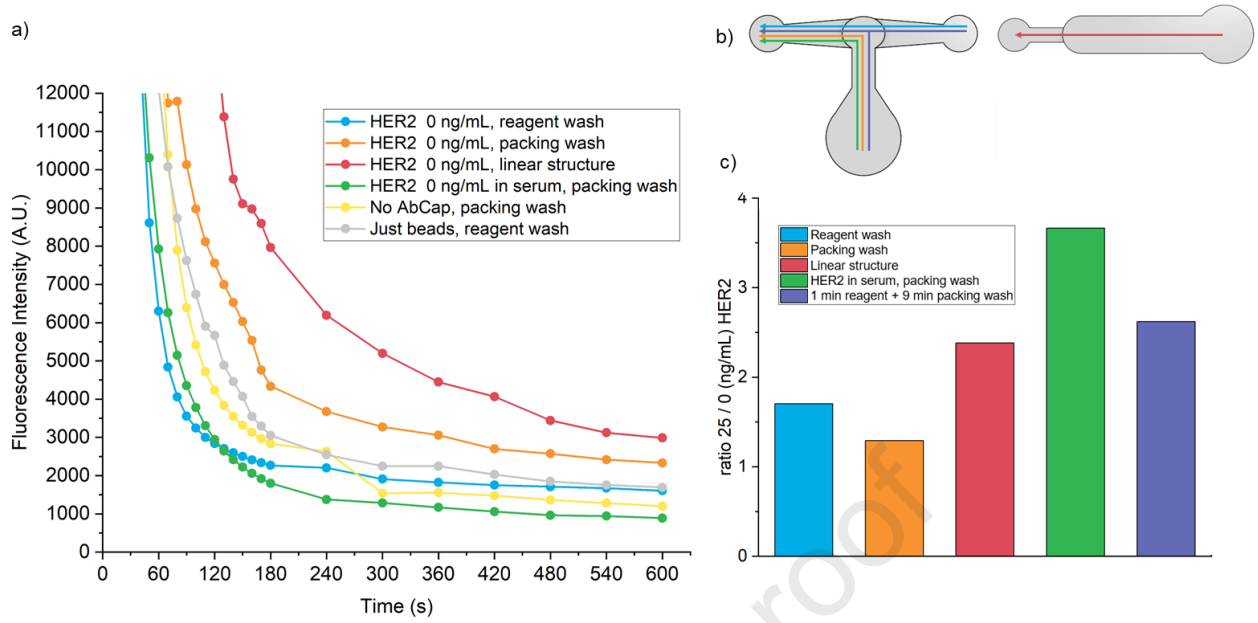

Figure 4 – Fluorescence intensity dependence on washing time for different washing and HER2 concentration conditions. All the images for fluorescence quantification were acquired in the bead chamber, the circular topmost region of the microfluidic channel. Colours represent the same washing conditions across subfigures. a) Washing curves comparing only HER2 0 ng/mL results. Each circle represents the mean of fluorescence intensity (A.U). b) Schematic of the washing conditions used. The structure on the right is the "linear" structure. c) Ratio between fluorescence intensity with HER2 test concentrations of 25 ng/mL and 0 ng/mL. In the bar chart, each column represents the ratio between the mean values of fluorescence intensity (A.U).

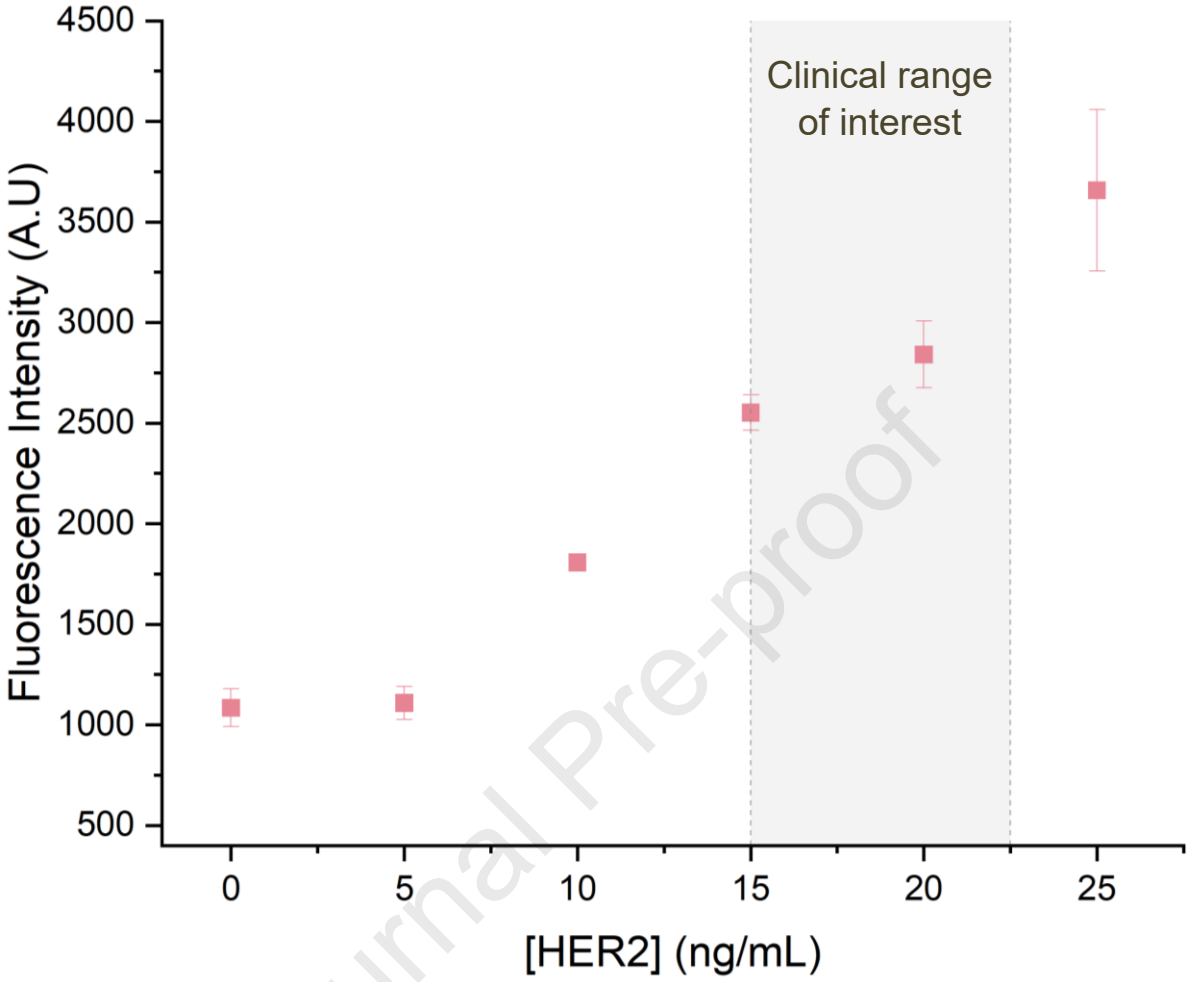

Figure 5 – Sensitivity curve for detection of HER2 in human serum. Each square represents the mean of fluorescence intensity (A.U) and the error bars are the standard deviation between replicas for each HER2 concentration. All the images for fluorescence quantification were acquired in the bead chamber, the circular topmost region of the microfluidic channel.

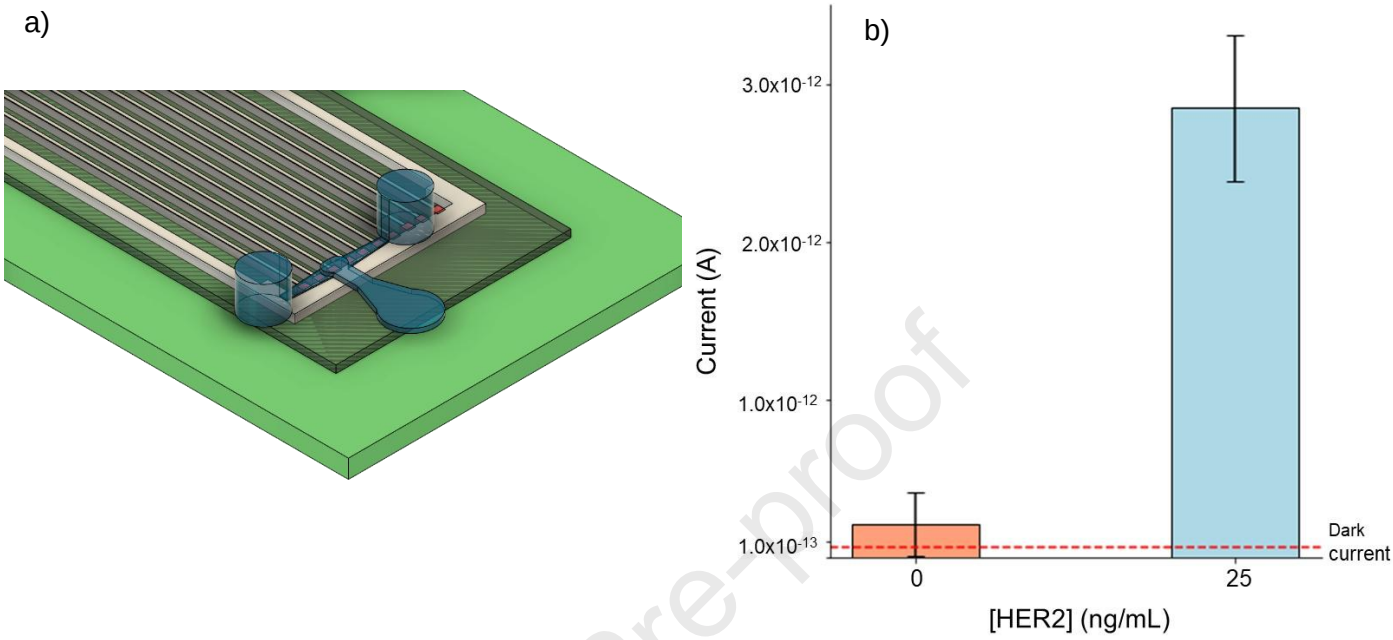

Figure 6 – Integrated fluorescence detection of HER2 in the microfluidic channel. a) Alignment of the microbead chamber of the microfluidic structure with the miniaturized thin-film silicon sensor in the linear sensor array. b) Photosensor output for HER2 concentrations of 0 and 25 ng/mL.

Table 1 - Comparison of representative HER2 biosensing platforms reported in the literature and the integrated fluorescence system presented in this work.

Representative HER2 biosensors spanning electrochemical, optical, and fluorescence modalities are compared in terms of analytical performance and degree of integration. “On-chip detection” denotes direct signal acquisition by an integrated sensor element within the device, while “Compact / POC-compatible” indicates architectural compatibility with portable or scalable implementations. The present platform uniquely combines bead-based antibody–aptamer recognition with thin-film a-Si:H photodiode fluorescence detection in a unified microfluidic architecture.

	Recognition Element	**Transduction Modality**	**LOD (approx.)**	**Linear Range**	**Sample Matrix**	**Approx. assay time**	**On-Chip Detection?**	**Compact / POC-Compatible?**	**Reference**
Electrochemical aptasensor (Au NP-modified electrode)	Aptamer	Electrochemical (volt.)	~0.001 ng/mL	~0.001–100 ng/mL	Buffer/serum	~10-15 min	No	Limited	[28]
Dual-signal electrochemical aptasensor	Aptamer	Dual-signal ratio electrochemical	~44.8 fg/mL	0.75–40 pg/mL	Buffer	~40-70 min (estimated)	No	Limited	[29]
Electrochemical aptasensor (screen-printed)	Aptamer	Electrochemical (DPV)	~3 ng/mL	~10–60 ng/mL	Serum (depleted)	~30-40 min (estimated)	No	Limited	[30]
Optical SPR biosensor	Antibody / Aptamer	Surface plasmon resonance	~pg/mL–ng/mL	Depends on platform	Plasma / buffer	~20-60 min	No	Moderate	[31]
Fluorescent HER2 sensor (MOF-based)	Aptamer / Fluorophore	Optical fluorescence	~6.67 pg/mL	0.01–10 ng/mL	Buffer	~30-60 min (estimated)	No	Limited	[32]
Fluorescence immunosensor (nanoparticle-based)	Antibody	Fluorescence (microscope)	Cell-level detection	Cells/mL	Cells	~1-2 hours	No	Low	[33]
This work	Antibody–Aptamer	Fluorescence (a-Si:H photodiode)	**7–8 ng/mL**	Clinically relevant	**90% human serum**	**~75 min**	**Yes**	**Yes**	—

Microfluidic fluorescence biosensor for quantitative detection of HER2 in serum using an antibody–aptamer sandwich assay

Research Highlights

- Fluorescence aptamer assay developed for detection of HER2 protein
- Integration of the sensing assay into a microfluidic platform
- Sensitive and selective HER2 detection using aptamer recognition
- Microfluidic format enables controlled handling of small sample volumes
- Platform shows potential for integrated biomarker sensing systems

Declaration of interests

☒ The authors declare that they have no known competing financial interests or personal relationships that could have appeared to influence the work reported in this paper.

☐ The authors declare the following financial interests/personal relationships which may be considered as potential competing interests: